Bioinformatic analysis and validation of cardiac hypertrophy-related genes

Ai Meng[1], Siang Wei[1], Lihuan Yan[1], Yao Xiao[1], Zhiwen Ding[2] and Yan Feng[1]

[1] *College of Life Science, Shanxi Agricultural University, Taigu, China*
[2] *Shanghai Municipal Institute for Cardiovascular Diseases, Zhongshan Hospital, Fudan University, Shanghai, China*

Abstract. In this study, we have screened genes involved in myocardial hypertrophy (MH) using a mice model for compensatory stress overload (transverse aortic constriction, TAC) and bioinformatics. Microarrays were downloaded, and according to the Venn diagram, three groups of data intersections were obtained. Gene function was analyzed by Gene Ontology (GO) and the Kyoto Encyclopedia of Genes and Genomes (KEGG), whereas protein-protein interactions (PPI) were analyzed using the STRING database. A mouse aortic arch ligation model was established to verify and screen the expression of hub genes. A total of 53 (DEGs) and 32 PPI genes were screened out. GO analysis showed DEGs mainly involved in cytokine and peptide inhibitor activity. KEGG analysis focused on ECM receptor interaction and osteoclast differentiation. Expedia co-expression gene network analysis showed that *Serpina3n*, *Cdkn1a*, *Fos*, *Col5a2*, *Fn1* and *Timp1* participated in the occurrence and development of MH. RT-qPCR verified that all the other 9 hub genes except *Lox* were highly expressed in TAC mice. This study lays a foundation for further study on the molecular mechanism of MH and for screening of molecular markers.

Key words: Cardiac hypertrophy — Target genes — Signaling pathway — Gene co-expression network — Protein-protein interaction — TAC mice

Introduction

The occurrence and development of cardiovascular disease is a complex process. Myocardial hypertrophy (MH) has one of the highest morbidities and mortalities. This is despite recent improvements in the understanding of MH pathogenesis and effective targeted therapies, which are essential to improve survival rates. MH has been known for over a century, but its molecular pathogenesis is still unclear. MH can be physiological, where cardiac enlargement is mainly caused by hypertrophy of cardiomyocytes during growth or exercise, or when dilated cardiomyocytes get sufficient nutrition due to capillary dilation (Shimizu and Minamino 2016). In pathological MH, in contrast, internal or external cardiovas-

cular damage, or pathogenic risk factors and gene mutations (such as hypertrophic cardiomyopathy) (Nakamura and Sadoshima 2018), cause structural and functional changes in the left ventricle (LV) and cardiac remodeling. Pathological remodeling is associated with fibrosis, inflammation and cellular dysfunction. Fibrosis increases the susceptibility of the heart to lethal arrhythmias (Radosinska et al. 2013; Egan et al. 2016). The pathophysiology of hypertrophy is complex and multifactorial (Samak et al. 2016). Understanding the molecular pathogenesis of MH is of great significance to protect the myocardium from pathological remodeling and delaying the occurrence of heart failure. Therefore, we have used bioinformatics methods to mine target molecules related to cardiac hypertrophy. This can expand the detection of biomarkers in patients with hypertrophic cardiomyopathy and prime further exploration in pathological MH.

MH animal can be established in several mammal species (Roth et al. 2017; Fu et al. 2020; Han et al. 2021), but

Correspondence to: Yan Feng, College of Life Science, Shanxi Agricultural University, 030801, Taigu, China
E-mail: fengyan0927@sina.com

mice are widely used because of their complete genetic background information, abundant commercial reagents, economical maintenance and easy feeding. Mice models of transverse aortic constriction (TAC) respond to post-load stress by initiating a series of altered gene expressions and activating complex crosstalk between signal pathways (Zhao et al. 2004). The present study selected three MH-related microarray data sets from the gene expression omnibus (GEO) database and analyzed them to determine differentially expressed genes (DEGs). Then, we systematically analyzed and discussed their potential functions and interaction mechanisms through bioinformatics methods and identified some molecules related to MH and signal pathways by RT-qPCR.

Materials and Methods

Laboratory animals

Ten 8–10-week-old male C57BL/6 mice weighing 19–25 g were bred in the Animal Breeding Center of Beijing Weishang Biological Co., Ltd. [SYXK (Beijing) 2016-0039]. The experiment was provided by Beijing Weishang Biological Co., Ltd. [SCXK (Beijing) 2016-0009]. There were five mice in the TAC group and five in the Control group. All mice were cared for humanely according to the principle of 3R (Beijing Weishang Biological Co., Ltd. Animal Experiment Animal Ethics Committee Approval No. 20200037).

Reagents and instruments

Reagents used were TRIzol (Shanghai Biyuntian Biotechnology Co., Ltd.), trichloromethane (Nitrogen Corporation), absolute ethanol (Sinopharm Chemical Reagent Co. Ltd.) PrimeScript^{TM} RT Reagent Kit (Nitrogen Corporation), SYBR Premix EX Taq^{TM} II (Takara Corporation of Japan), and equipment used was PCR Amplification Instrument (Applied Biological Systems Corporation of America), QuantStudio^{TM} Real-Time PCR (Thermo Fisher Technology Co. Ltd.) and a small animal ventilator (Harvard Corporation of America).

Experimental methods

Data acquisition

Three datasets from MH tissues were identified and screened out from the GEO database, which had both MH and normal control tissue: GSE18801 (platform: GPL1261), GSE120739 (platform: GPL6887), and GSE26671 (platform: GPL1261). MH and normal control tissue samples were taken from mice. MH was induced in mice with isoproterenol of the GSE18801 data set (Galindo et al. 2009). Isoproterenol alters several genes that are involved in the acute phase and oxi-

dative stress response signaling of myocardial hypertrophy, which is associated with maladaptive cardiac remodeling (Heineke and Molkentin 2006; Barry et al. 2008). MH tissues in GSE120739 and GSE26671 datasets were obtained by TAC (Zhang et al. 2018). This treatment leads to compensated hypertrophy of the heart, often associated with temporary enhancement of cardiac contractility. Over time, however, the response to this chronic hemodynamic overload becomes maladaptive and results in cardiac dilation and heart failure. The DEGs between normal heart and MH tissue were identified by the GEO2R tool setting the filters to |log 2 FC| ≥ 1, $p \le 0.05$, where FC is the fold change.

Detection of samples and determination of cross-fertile DEGs

Volcano plots and Venn diagrams were obtained with SaneBox software (http://vip.sangerbox.com/) (Shen et al. 2022) and Venn Diagram online software. The DEGs at intersections pointed to three data sets that were used for subsequent analysis.

GO enrichment and KEGG pathway analyses

GO enrichment of DEGs was analyzed by DAVID (http://david.ncifcrf.gov) (Dennis et al. 2003). Understanding molecular function (MF) involves biological process (BP), cellular component (CC) and analysis of the KEGG pathway. $p < 0.05$ was used as the inclusion criteria.

PPI network construction and hub gene module analysis

Information from DEGs was extracted from the STRING database (https://cn.string-db.org/) (Mering et al. 2003). A network of PPIs was constructed and visualized using Cytoscape 3.7.2. The molecular complex detection (MCODE) plug-in selected essential modules and genes in the network. MCODE score and number of nodes were both set to be greater than five, and $p \le 0.05$ was considered to be significantly different.

Co-expression analysis and phenotype analyses of hub genes

Expedia website and phenotypic analysis of the top ten essential genes were used to analyze hub genes and their co-expression networks obtained from the PPI network.

Validation of hub gene mRNA expression

The MH mouse was established as follows: the transverse aorta was constricted at the upper left sternal border by ligation with a 7-silk surgical thread and a 27-gauge needle, which was removed thereafter. Sham-operated controls underwent an identical procedure without TAC. Samples were taken 1 month after the operation (deAlmeida et al. 2010). After cervi-

Table 1. Primer sequences

Gene name	Primer sequence
GAPDH	F: AGGTCGGTGTGAACGGATTTG R: GGGGTCGTTGATGGCAACA
Timp1	F: GCAACTCGGACCTGGTCATAA R: CGGCCCGTGATGAGAAACT
Ctgf	F: GGGCCTCTTCTGCGATTTC R: ATCCAGGCAAGTGCATTGGTA
Serpina3n	F: ATTTGTCCCAATGTCTGCGAA R: TGGCTATCTTGGCTATAAAGGGG
Cp	F: CTTAGCCTTGGCAAGAGATAAGC R: GGCCTAAAAACCCTAGCCAGG
Cdkn1a	F: CCTGGTGATGTCCGACCTG R: CCATGAGCGCATCGCAATC
Fos	F: CGGGTTTCAACGCCGACTA R: TTGGCACTAGAGACGGACAGA
Spp1	F: AGCAAGAAACTCTTCCAAGCAA R: GTGAGATTCGTCAGATTCATCCG
Col5a2	F: TTGGAAACCTTCTCCATGTCAGA R: TCCCCAGTGGGTGTTATAGGA
Fn1	F: ATGTGGACCCCTCCTGATAGT R: GCCCAGTGATTTCAGCAAAGG

F, forward; R, reverse

cal dislocation, mice were cut open at the chest and the heart was perfused with 2–3 ml of saline. The left atrial ear and other redundant tissues were removed and the loose tissue was put on gauze to dry. Hypertrophic tissues were stored at −80°C. Primers were synthesized by Shanghai Qingke Biotechnology Co., Ltd (Table 1). Gene amplification was calculated using a two-step method, and the relative expression was calculated using the $2^{-\Delta\Delta Ct}$ method. For the Masson staining, mouse hearts were fixed and labeled, and Masson staining was carried out according to Schipke et al. (2017).

Statistical analysis

GraphPad Prism (Swift 1997) was used for statistical analysis. Results were expressed as mean ± standard deviation. Comparison between datasets was performed by one-way ANOVA, with significance * $p < 0.05$, ** $p < 0.01$ or *** $p \leq 0.0001$.

Results

Identification of MH DEGs

We used gene datasets with normal (N) and MH mice: GSE18801 (3N + 3MH), GSE120739 (1N + 2 MH) and GSE26671 (2N + 2MH). Three Volcano Plot datasets were drawn (Fig. 1A–C). Green and red indicate upregulated and downregulated genes, respectively. To establish a mouse model of cardiac hypertro-

phy, TAC mice were used. DEGs were screened by comparing hypertrophic tissue with normal samples, and 53 genes were visualized using a Venn diagram (Fig. 1D).

GO enrichment analysis of DEGs

DEGs were closely related to fibronectin binding, heparin-binding, actin-binding, protease binding, FK506 binding, oxidoreductase activity, Wnt protein binding, and other aspects. The biological processes involved are mainly the positive regulation of fibroblast proliferation, cellular adhesion, wound healing, active oxygen metabolism, extracellular matrix tissue, angiogenesis, collagen fiber tissue, aging, cell proliferation, peptide hormone reaction, and negative regulation of apoptosis. DEGs were significantly enriched in the extracellular domain, extracellular matrix, extracellular space, extracellular matrix, collagen trimer, basement membrane, exosome, Z-disk, stress fiber, microfibril, and perinuclear region of cytoplasm, endoplasmic reticulum membrane, blood particles, neuronal processes, and the actin cytoskeleton. The following table lists the partial GO enrichment analysis (Table 2).

Enrichment analysis of the KEGG pathway

KEGG pathway analysis showed that DEGs were mainly enriched in seven signal pathways: extracellular matrix (ECM) receptor interaction, osteoclast differentiation, tuberculosis, PI3K-Akt signaling pathway, adhesion plaque,

Table 2. Partial GO enrichment analyses of DEGs

	Description	Count	p-value
BP	Positive regulation of fibroblast	4	3.19E−4
	Inflammatory response	7	3.67E−4
	Collagen fibril organization	4	3.72E−4
	Extracellular matrix organization	5	5.89E−4
	Cell adhesion	7	1.781E−3
CC	Extracellular region	20	3.25E−8
	Extracellular matrix	8	1.44E−6
	Extracellular space	16	9.09E−6
	Collagen trimer	5	4.94E−5
	Stress fiber	6	5.41E−4
MF	Extracellular matrix structural constituent	7	1.03E−6
	Integrin binding	4	7.135E−4
	Actin binding	5	9.324E−4
	Collagen binding	3	1.2029E−2
	FK506 binding	2	2.4192E−2

GO, Gene Ontology; DEGs, differentially expressed genes; BP, biological process; CC, cellular component; MF, molecular function.
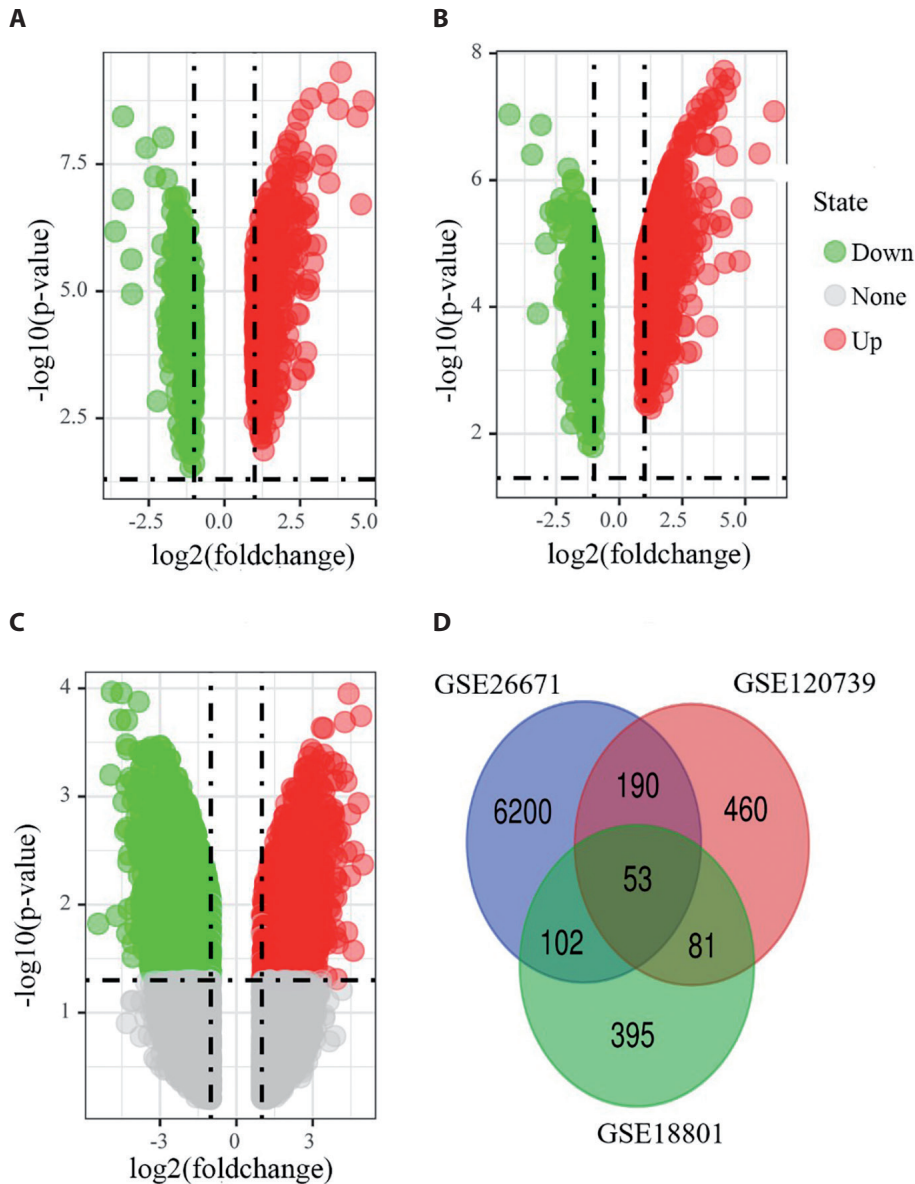
Figure 1. Gene analysis of myocardial hypertrophy differential expression. GSE18801 (**A**), GSE120739 (**B**), GSE26671 (**C**) and Venn results of DEGs from the three datasets (**D**).

estrogen signaling pathway and Toll-like receptor signaling pathway (Fig. 2). Four genes were involved in ECM receptor interaction ($p = 0.003$), 4 genes involved in osteoclast differentiation ($p = 0.009$), 4 genes related to tuberculosis ($p = 0.02$), 5 genes were involved in PI3K-Akt signaling pathway ($p = 0.003$), 4 genes were involved in adhesive plaque ($p = 0.03$), 3 genes were involved in estrogen signaling pathway ($p = 0.045$), and 3 genes were involved in toll-like receptor signaling pathway ($p = 0.048$).

PPI network construction and key module selection

To further study the role of DEGs on MH, 32 proteins obtained from the STRING database were used to con-

struct a PPI network using Cytoscape software, which combined 32 nodes and 59 edges (Fig. 3A). Ten essential genes selected using the PPI network and obtained the first necessary modules composed of 10 nodes and 30 edges (Fig. 3B).

Expression network and phenotypic analysis of hub genes

Expedia (http://www.coexpedia.org/) analyzed ten essential genes and their co-expression networks, selecting species as mouse, and a score >10 (Fig. 4). Phenotypic analysis showed that these ten hub genes participated in 298 mammalian phenotypes, and the *p*-value of the enrichment term was less than 0.05 (Table 3).

MH mouse model

The weights of TAC mice were not significantly different from those in the Control group, but the heart and left ventricle were heavier than in the Control (Table 4). The *BNP* gene was highly expressed in cardiac hypertrophy caused by pressure overload; expression of *BNP* mRNA in TAC mice was significantly higher than in sham-operated mice ($p < 0.01$), indicating that the MH mouse model was successfully established and could be used to screen and detect biomarkers of myocardial hypertrophy (Fig. 5). The papillary 20× (Fig. 6A) and 40× (Fig. 6B) upright microscope normal and TAC mouse sliced field of view shows that there was an increase of fibrosis in hypertrophic heart slices, whereas myocardial cells were larger than in standard mice.

Hub gene validation results

After successfully generating a mouse myocardial hypertrophy model, the genes obtained from the PPI network were verified in all cases (Fig. 7), except *Lox*, because its primer had low specificity and therefore it was not suitable for RT-PCR. Compared with the sham-operation group, the relative mRNA expression of *Timp1* in the hypertrophic group was 9.54 times ($p < 0.0001$), *Ctgf* was 3.74 times ($p < 0.0001$), *Serpina3n* was 12.13 times ($p < 0.0001$), *Cp* was 3.44 times ($p < 0.0001$), *Cdkn1a* was 1.86 times ($p < 0.05$), *Fos* was
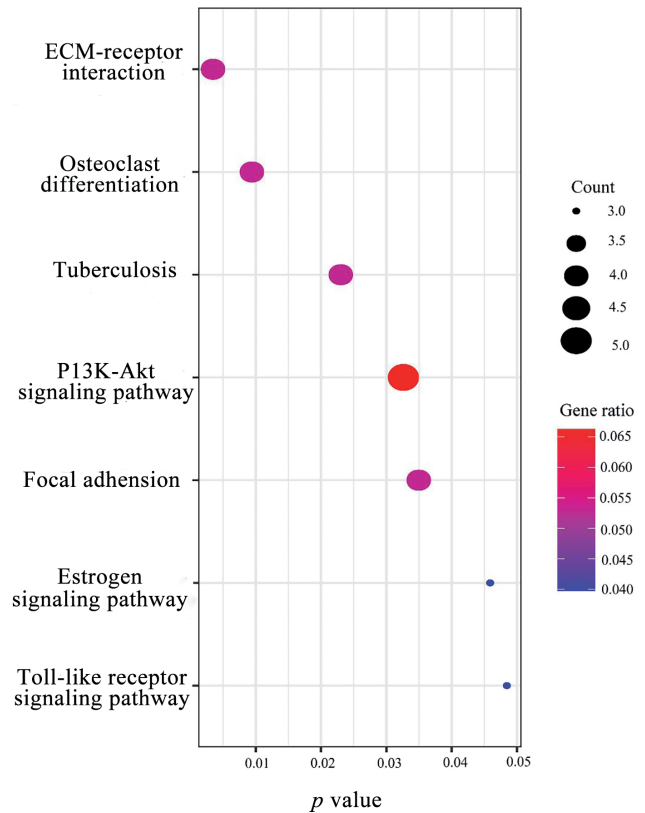

Figure 2. Signal pathways involved in the enrichment of DEGs. ECM, extracellular matrix.
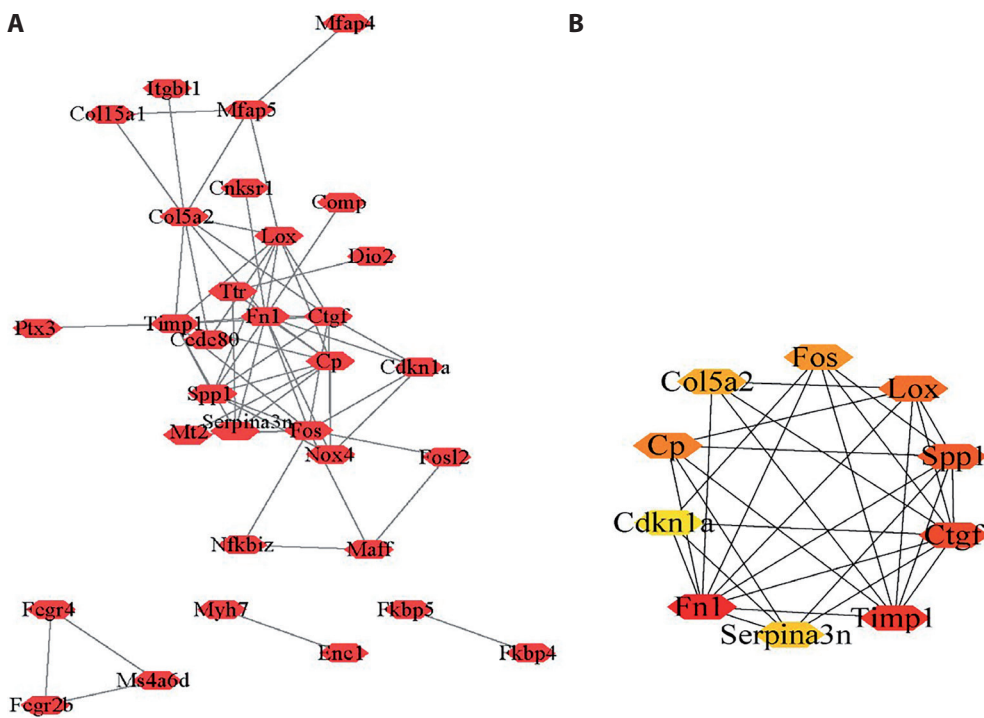

Figure 3. Protein-protein interaction network and gene module with the highest degree of tight connections. Interaction network of 32 DEGs (**A**) and Gene modules with the highest degree of tight junctions (**B**).
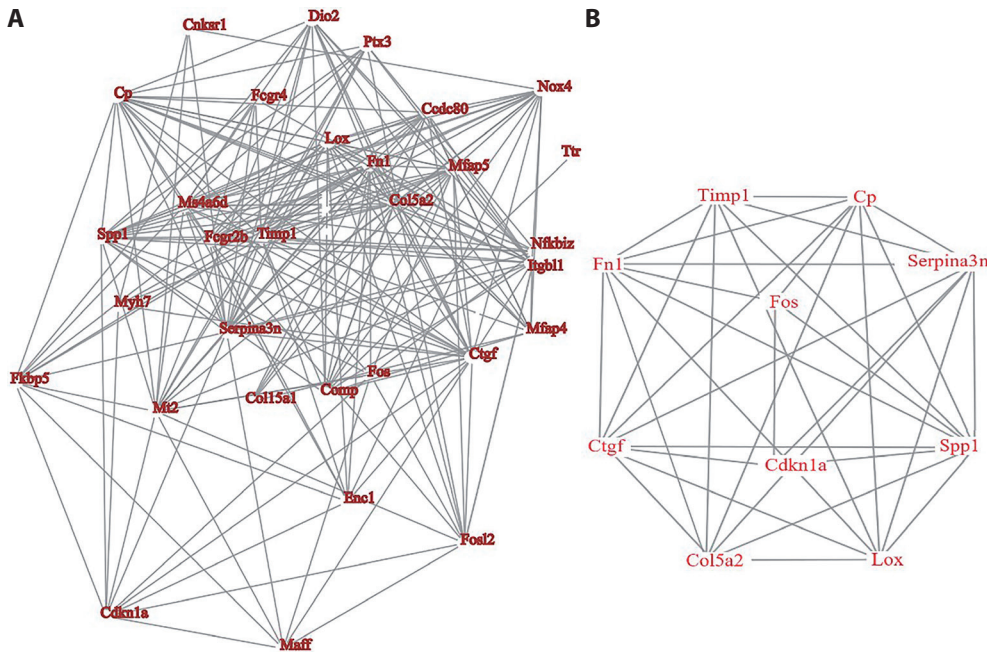
A

B

Figure 4. Co-expression network of myocardial hypertrophy-related genes. DEGs co-expression network (**A**) and TOP10 gene co-expression block (**B**).

3.06 times ($p < 0.0001$), *Spp1* was 16.63 times ($p < 0.0001$), *Col5a2* was 3.26 times ($p < 0.0001$), and *Fn1* was 3.42 times ($p < 0.0001$). Nine DEGs of MH were screened out, and they participated in the occurrence of MH.

Discussion

Although several recent studies have shown that DEGs are important in human MH, their specific function is un-

Table 3. Some phenotypic effects of Hub genes in mammals

| Rank	MGI MP ID	Name	*p*-value
1	MP:0006278	Aortic aneurysm	8.618E−8
2	MP:0005341	Decreased susceptibility to atherosclerosis	1.170E−6
3	MP:0005164	Abnormal response to injury	1.626E−6
4	MP:0008469	Abnormal protein level	1.473E−5
5	MP:0000585	Kinked tail	2.372E−5
6	MP:0000233	Abnormal blood flow velocity	3.410E−5
7	MP:0003089	Decreased skin tensile strength	5.142E−5
8	MP:0008438	Abnormal cutaneous collagen fibril morphology	5.142E−5
9	MP:0005631	Decreased lung weight	6.141E−5
10	MP:0008947	Increased neuron number	7.227E−5
11	MP:0000131	Abnormal long bone epiphysis morphology	8.401E−5
12	MP:0008874	Decreased physiological sensitivity to xenobiotic	8.699E−5
13	MP:0000249	Abnormal blood vessel physiology	9.021E−5
14	MP:0004771	Increased anti-single stranded DNA antibody level	9.663E−5
15	MP:0006397	Disorganized long bone epiphyseal plate	1.033E−4
16	MP:0000761	Thin diaphragm muscle	1.245E−4
17	MP:0001209	Spontaneous skin ulceration	1.816E−4
18	MP:0008102	Lymph node hyperplasia	1.907E−4
19	MP:0004321	Short sternum	1.999E−4
20	MP:0010300	Increased skin tumor incidence	2.190E−4
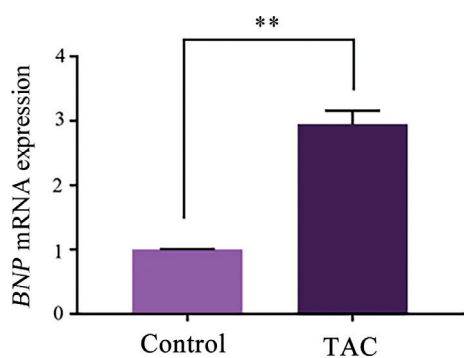
Figure 5. Validation of transverse aortic constriction (TAC) mouse model. ** *p* < 0.01 significant *vs*. Control group.

clear. We screened ten hub genes with a score greater than ten and established a TAC-induced MH mouse model to verify the presence of DEGs in hypertrophic myocardium to understand the mechanisms of compensatory myocardial hypertrophy caused by stress overload. The high expression of these genes, except *Lox*, in hypertrophic cardiomyopathy mice is consistent with their known activation of signaling pathways in various types of cardiac hypertrophy. For example, AMPK-mTOR is a signal transduction pathway leading to pathological MH, whereas JMJD1C is involved in MH through this pathway (Yu et al. 2020). The latest research shows that JMJD1C can up-regulate *Timp1*, thereby

promoting cardiac hypertrophy and fibrosis (Zhang et al. 2020). Therefore, *Timp1* may be involved in pathological MH through this pathway. *CTF* is a promoter of cardiac fibrosis therefore its high expression should aggravate it (Dorn et al. 2018), consistent with our Masson staining results. Expression of *Serpina3n* increases after pressure overload (Gao et al. 2018), which indicates its involvement in MH pathogenesis since it is related to vasoconstriction and blood pressure increase (Arenas de Larriva et al. 2020). *Cp* may induce MH through ferroptosis since it is a critical factor in this signaling pathway and it is highly expressed in the serum of patients with hypertension, coronary heart disease and myocardial infarction. *Cdkn1a* was highly expressed in TAC mice, although not as significantly as other DEGs. *Cdkn1a* is an effective inhibitor of cyclin-dependent kinase, binding to cyclin-dependent enzyme 2 or cyclin-dependent kinase 4 complex, thus regulating the progress of the G1 phase cell cycle. *Cdkn1a* interacts with DNA polymerase cofactor proliferating nuclear antigens and plays a regulatory role in S-phase DNA replication and damage repair (Alila-Fersi et al. 2018). Thus, an increase in *Cdkn1a* may contribute to repair the missing mitochondrial DNA fragment in MH (Zhang et al. 2016). The observed increase in expression of *Fn1* and *Spp1* is linked to fibrosis of hypertrophic hearts, consistent with our results. Indeed, Palomer et al. (2020) found that *Sirt3* inhibits *Fos* and prevents cardiac fibrosis and inflammation, while the high *Fos* expression observed herein confirms its essential role in myocardial fibrosis. Finally, *Col5a2* is
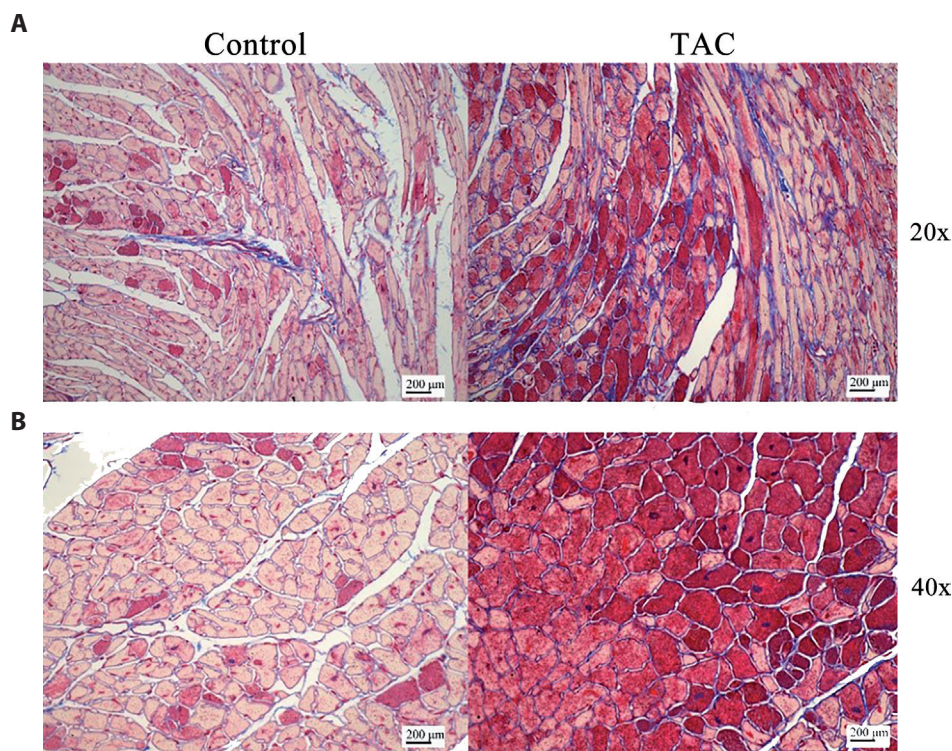

Figure 6. Masson staining results in papillary muscle. Papillary muscles of normal (Control) and transverse aortic constriction (TAC) mice under 20× (**A**) and 40× (**B**) visual field.

Table 4. Basic biological characteristic parameters of Control and TAC group of mice

Group	BW (g)	BW/TL (g/cm)	HW (g)	HW/TL (g/cm)	Left ventricle (mg)
Control	24.2 ± 1.402	7.174 ± 0.449	0.128 ± 0.0217	0.038 ± 0.006	0.13 ± 0.01
TAC	23.56 ± 1.016	7.034 ± 0.46	0.16 ± 0.007*	0.048 ± 0.002**	0.15 ± 0.012*

Date are mean ± SEM of 5 animals *per* group. * $p < 0.05$, ** $p < 0.01$ *vs.* Control group. BW, body weight; TL, the length of mouse tibia; HW, heart weight; TAC, transverse aortic constriction.
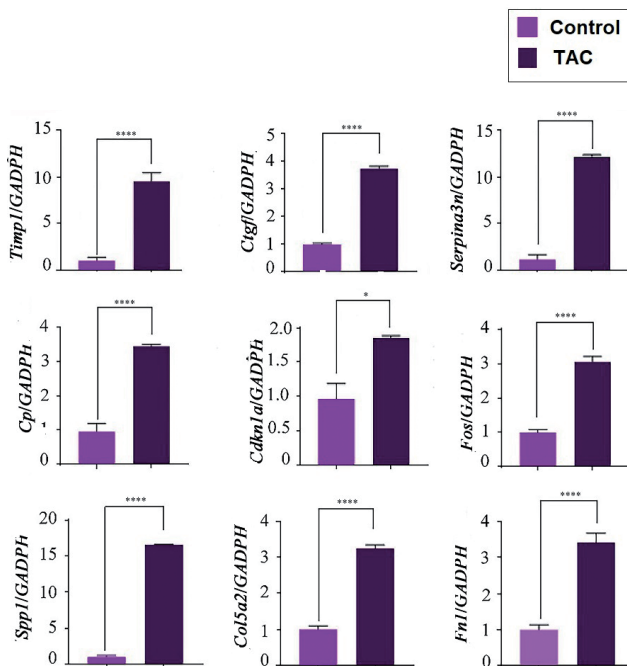

Figure 7. Relative gene expression of *Timp1*, *Ctgf*, *Serpina3n*, *Cp*, *Cdkn1a*, *Fos*, *Spp1*, *Col5a2*, and *Fn1* in myocardial hypertrophy screening by RT-qPCR. * $p < 0.05$, **** $p < 0.0001$ significant *vs.* Control group. TAC, transverse aortic constriction mice.

linked to the maintenance of the function of the heart valve (Peacock et al. 2008), which may explain its high expression caused by the thickening of the heart valve in MH.

Conclusion

In summary, using bioinformatics we systematically discussed the role of DEGs in the occurrence and development of MH. We screened and identified ten critical genes that may be involved in MH and cardiac remodeling. These results contribute to delineate MH pathogenesis and to develop therapeutic targets and prognostic molecular markers.

References

Alila-Fersi O, Tabebi M, Maalej M, Belguith N, Keskes L, Mkaouar-Rebai E, Fakhfakh F (2018): First description of a novel mitochondrial mutation in the MT-TI gene associated with multiple mitochondrial DNA deletion and depletion in family with severe dilated mitochondrial cardiomyopathy. Biochem. Biophys. Res. Commun. **497,** 1049-1054
https://doi.org/10.1016/j.bbrc.2018.02.173

Arenas de Larriva AP, Limia-Pérez L, Alcalá-Díaz JF, Alonso A López-Miranda, J, Delgado-Lista J (2020): Ceruloplasmin and coronary heart disease - a systematic review. Nutrients **12,** 3219
https://doi.org/10.3390/nu12103219

Barry SP, Davidson SM, Townsend PA (2008): Molecular regulation of cardiac hypertrophy. Int. J. Biochem. Cell Biol. **40,** 2023-2039
https://doi.org/10.1016/j.biocel.2008.02.020

deAlmeida AC, van Oort RJ, Wehrens XH (2010): Transverse aortic constriction in mice. JoVE (Journal of Visualized Experiments). **2020,** e1729
https://doi.org/10.3791/1729

Dennis G, Sherman BT, Hosack DA, Yang J, Gao W, Lane HC, Lempicki RA (2003): DAVID: database for annotation, visualization, and integrated discovery. Genome Biol. **4,** 1-11
https://doi.org/10.1186/gb-2003-4-9-r60

Dorn LE, Petrosino JM, Wright P, Accornero F (2018): CTGF/CCN2 is an autocrine regulator of cardiac fibrosis. J. Mol. Cell. Cardiol. **121,** 205-211
https://doi.org/10.1016/j.yjmcc.2018.07.130

Egan Benova T, Szeiffova BB, Viczenczova C, Diez ER, Barancik M, Tribulova N (2016): Protection of cardiac cell-to-cell coupling attenuate myocardial remodeling and proarrhythmia induced by hypertension. Physiol. Res. **65,** 29-42
https://doi.org/10.33549/physiolres.933391

Fu DT, Tu J, Cai YQ, Cai ZW, Zhang LZ, Liu JY, Xu SC, Wang DJ (2020): The regulatory mechanism of Raf/MEK/ERK pathway on the rat cardiac hypertrophy induced by transverse aortic constriction. Zhongguo Ying Yong Sheng Li Xue Za Zhi **36,** 33-38 (in Chinese)

Galindo CL, Skinner MA, Errami M, Olson LD, Watson DA, Li J, McCormick JF, McIver LJ, Kumar NM, Pham TQ, et al. (2009): Transcriptional profile of isoproterenol-induced cardiomyopathy and comparison to exercise-induced cardiac hypertrophy and human cardiac failure. BMC Physiology **9,** 1-22
https://doi.org/10.1186/1472-6793-9-23

Gao J, Li Y, Wang T, Shi Z, Zhang Y, Liu S, Wen P, Ma C (2018): Analyzing gene expression profiles with preliminary validations in cardiac hypertrophy induced by pressure overload. Can. J. Physiol. Pharmacol. **96,** 701-709
https://doi.org/10.1139/cjpp-2017-0585

Han Z, Bi S, Xu Y, Dong X, Mei L, Lin H, Li X (2021): Cholecystokinin expression in the development of myocardial hypertrophy. Scanning **2021,** 8231559
https://doi.org/10.1155/2021/8231559

Heineke J, Molkentin JD (2006): Regulation of cardiac hypertrophy by intracellular signalling pathways. Nat. Rev. Mol. Cell Biol. **7,** 589-600
https://doi.org/10.1038/nrm1983

Mering CV, Huynen M, Jaeggi D, Schmidt S, Bork P, Snel B (2003): STRING: a database of predicted functional associations between proteins. Nucleic Acids Res. **31,** 258-261
https://doi.org/10.1093/nar/gkg034

Nakamura M, Sadoshima J (2018): Mechanisms of physiological and pathological cardiac hypertrophy. Nat. Rev. Cardiol. **15,** 387-407
https://doi.org/10.1038/s41569-018-0007-y

Palomer X, Román-Azcona MS, Pizarro-Delgado J, Planavila A, Villarroya F, Valenzuela-Alcaraz B, Crispi F, Sepúlveda-Martínez Á, Miguel-Escalada I, Ferrer J (2020): SIRT3-mediated inhibition of FOS through histone H3 deacetylation prevents cardiac fibrosis and inflammation. Signal Transduct. Target. Ther. **5,** 1-10
https://doi.org/10.1038/s41392-020-0114-1

Peacock JD, Lu Y, Koch M, Kadler KE, Lincoln J (2008): Temporal and spatial expression of collagens during murine atrioventricular heart valve development and maintenance. Dev. Dyn. **237,** 3051-3058
https://doi.org/10.1002/dvdy.21719

Radosinska J, Bacova B, Knezl V, Benova T, Zurmanova J, Soukup T, Arnostova P, Slezak J, Gonçalvesova E, Tribulova N (2013): Dietary omega-3 fatty acids attenuate myocardial arrhythmogenic factors and propensity of the heart to lethal arrhythmias in a rodent model of human essential hypertension. J. Hypertens. **31,** 1876-1885
https://doi.org/10.1097/HJH.0b013e328362215d

Roth GA, Johnson C, Abajobir A, Abd-Allah F, Abera SF, Abyu G, Roth GA, Johnson C, Abajobir A, Abd-Allah F, et al. (2017): Global, regional, and national burden of cardiovascular diseases for 10 causes, 1990 to 2015. J. Am. Coll. Cardiol. **70,** 1-25

Samak M, Fatullayev J, Sabashnikov A, Zeriouh M, Schmack B, Farag M, Popov AF, Dohmen PM, Choi YH, Wahlers T (2016): Cardiac hypertrophy, an introduction to molecular and cellular basis. Med. Sci. Monit. Basic Res. **22,** 75
https://doi.org/10.12659/MSMBR.900437

Schipke J, Brandenberger C, Rajces A, Manninger M, Alogna A, Post H, Mühlfeld C (2017): Assessment of cardiac fibrosis, a morphometric method comparison for collagen quantification. J. Appl. Physiol. **122,** 1019-1030
https://doi.org/10.1152/japplphysiol.00987.2016

Shen W, Song Z, Zhong X, Huang M, Shen D, Gao P, Qian X, Wang M, He X, Wang T, et al. (2022): Sangerbox: A comprehensive, interaction-friendly clinical bioinformatics analysis platform. iMeta **1,** e36
https://doi.org/10.1002/imt2.36

Shimizu I, Minamino T (2016): Physiological and pathological cardiac hypertrophy. J. Mol. Cell. Cardiol. **97,** 245-262
https://doi.org/10.1016/j.yjmcc.2016.06.001

Swift ML (1997): GraphPad prism, data analysis, and scientific graphing. J. Chem. Inf. Comput. Sci. **37,** 411-412
https://doi.org/10.1021/ci960402j

Yu S, Li Y, Zhao H, Wang Q, Chen P (2020): The histone demethylase JMJD1C regulates CAMKK2-AMPK signaling to participate in cardiac hypertrophy. Front. Physiol. **11,** 539
https://doi.org/10.3389/fphys.2020.00539

Zhang C, Wu M, Zhang L, Shang LR, Fang JH, Zhuang SM (2016): Fibrotic microenvironment promotes the metastatic seeding of tumor cells via activating the fibronectin 1/secreted phosphoprotein 1-integrin signaling. Oncotarget **7,** 45702
https://doi.org/10.18632/oncotarget.10157

Zhang QJ, Tran TA T, Wang M, Ranek MJ, Kokkonen-Simon KM, Gao J, Luo X, Tan W, Kyrychenko V, Liao L, et al. (2018): Histone lysine dimethyl-demethylase KDM3A controls pathological cardiac hypertrophy and fibrosis. Nat. Commun. **9,** 1-12
https://doi.org/10.1038/s41467-018-07173-2

Zhang S, Lu Y, Jiang C (2020): Inhibition of histone demethylase JMJD1C attenuates cardiac hypertrophy and fibrosis induced by angiotensin II. J. Recept. Signal Transduct. Res. **40,** 339-347
https://doi.org/10.1080/10799893.2020.1734819

Zhao M, Chow A, Powers J, Fajardo G, Bernstein D (2004): Microarray analysis of gene expression after transverse aortic constriction in mice. Physiol. Genomics **19,** 93-105
https://doi.org/10.1152/physiolgenomics.00040.2004